

The adsorption of CO on group 10 (Ni, Pd, Pt) transition-metal clusters

Philipp Gruene,^a André Fielicke,^{*a} Gerard Meijer^a and David M. Rayner^{*b}

Received 16th May 2008, Accepted 30th June 2008

First published as an Advance Article on the web 5th September 2008

DOI: 10.1039/b808341j

The adsorption of a single CO molecule on clusters of the Group 10 transition metals is characterized by infrared multiple photon dissociation (IR-MPD) spectroscopy. The cationic, neutral, and anionic carbonyl complexes contain between 3 and up to 25 metal atoms. The C–O stretching frequency $\nu(\text{CO})$ shows that while both nickel and platinum clusters adsorb CO only in atop positions, palladium clusters exhibit a variety of binding sites. These findings can be rationalized by considering the increasing role relativistic effects play in the electronic structure of the cluster complexes going down the group. Conclusions for the cluster-support interactions for size-selected supported particles are drawn from the charge dependence of $\nu(\text{CO})$ for the gas-phase species.

I. Introduction

By identifying and understanding relativistic effects in the chemistry of transition-metal clusters we hope to provide better insight into factors governing transition metal centered chemistry and heterogeneous catalysis. Relativistic effects lead to a contraction and stabilization of atomic s and p orbitals, while the d and f orbitals expand radially and increase in energy.¹ This modification in the electronic structure can result in marked changes concerning the structural properties² as well as the reactivity³ of compounds of heavy elements, and thus has consequences for both homogeneous⁴ and heterogeneous catalysis.⁵ Many proven catalysts are based on second and third row transition metals. Clusters are relevant in this respect for two reasons. Firstly, size-selected deposited clusters are under investigation as the basis for a new generation of rationally designed catalysts.⁶ Secondly, cluster models are regularly employed in attempts to calculate the behaviour of extended metal surfaces. Experimental information on free clusters allows direct validation of the theoretical methods used in this approach.

Here we make a comparative study of CO adsorption on free clusters of the Group 10 metals nickel, palladium, and platinum. We use vibrational spectroscopy to determine the nature of the CO binding sites. The relativistic contraction of the 6s orbital of platinum is the largest of all stable elements after gold.⁷ Consequently we can expect CO adsorption on platinum clusters to be significantly influenced by relativistic effects. This should be reflected in the C–O stretching frequency $\nu(\text{CO})$ that is highly sensitive to the nature of the binding site and its electronic configuration. Relativistic effects may be recognized by comparison to the lighter members of the group.

From an applied perspective, especially palladium and platinum are of pronounced importance regarding CO oxidation as reflected by their use in catalytic converters. Despite its industrial relevance, CO adsorption on such species is not yet fully understood. On extended platinum surfaces CO adsorbs in atop positions. While some theoretical studies have identified relativistic effects as the cause of this adsorption behaviour,^{8,9} density functional theory (DFT) calculations still have problems in predicting the right adsorption site for CO on platinum surfaces.¹⁰ Complexes of small transition-metal clusters with carbon monoxide represent valuable benchmark systems for a better understanding of catalytically relevant reaction intermediates.

We measure $\nu(\text{CO})$ using infrared multiple photon dissociation (IR-MPD) spectroscopy. Using this method, insights into the binding geometry of CO on transition-metal clusters, as well as the charge dependence of $\nu(\text{CO})$ have been gained for rhodium,^{11–13} nickel, cobalt,¹³ and gold clusters.^{14–16} Here we show that the trend from atop, μ_1 , binding on nickel towards bridge, μ_2 , and hollow-site, μ_3 , binding on palladium clusters is reversed for platinum. The latter demonstrates only μ_1 binding.

II. Experimental

The experiments are performed using two similar molecular beam setups coupled to beamlines of the Free Electron Laser for Infrared eXperiments (FELIX).¹⁷ The use of FELIX for IR spectroscopy of cluster–ligand complexes has been described in detail earlier.^{12,18} While one instrument is equipped with a pulsed-valve source, a new molecular beam setup is equipped with a continuous flow source as described in the literature.¹⁹ In both instruments metal vapour is generated upon pulsed laser ablation of a rotating metal rod using the 2nd harmonic output of a Nd:YAG laser. The metal atoms condense in a short He pulse or in a continuous He flow (typically 1500–2500 standard cubic centimetres per minute), respectively. Clusters are formed and travel down a reaction channel where CO is introduced downstream of the source. In

^a Fritz-Haber-Institut der Max-Planck-Gesellschaft, Faradayweg 4-6, D-14195 Berlin, Germany.

E-mail: fielicke@fhi-berlin.mpg.de

^b Steacie Institute for Molecular Sciences, National Research Council, 100 Sussex Drive Ottawa, Ontario, Canada K1A 0R6.

E-mail: david.rayner@nrc-cnrc.gc.ca

these experiments the CO pressure is adjusted to produce predominantly complexes with only a single CO molecule adsorbed. The molecular beam passes through a skimmer and an aperture of 1 mm in diameter into the detection chamber, where the ions are accelerated between the pulsed extraction plates of a reflectron time-of-flight mass spectrometer (TOF-MS, Jordan TOF Products). In order to study neutral complexes, a DC potential is applied to the aperture to deflect all ionic species from the beam. The neutral species are subsequently ionized between the extraction plates of the mass spectrometer using an F₂ excimer laser (7.9 eV photon⁻¹), with the laser fluence kept sufficiently low to avoid fragmentation induced by UV multiple photon absorption.

The IR beam delivered by FELIX counter-propagates the cluster beam and is loosely focused to cover the aperture through which the cluster beam enters the ion detection region of the TOF-MS. This ensures that the full cross section of the cluster beam which is detected is exposed to the IR laser beam. Spectra are recorded with IR pulse energies of up to 20 mJ at 2000 cm⁻¹. The length of a macro pulse is about 5 μs. In the CO stretching region FELIX frequencies are calibrated by recording the infrared absorption spectra of ethylene and CO in a photoacoustic cell. When the IR radiation is in resonance with the C–O stretch vibration $\nu(\text{CO})$ of molecularly adsorbed carbon monoxide on a metal cluster, photons can be absorbed sequentially. This leads to heating of the cluster and eventually to the evaporation of the CO ligand. The evaporation of CO from the cluster results in a decrease of the mass spectrometric signal of the cluster complex and in an enhancement of the signal of the bare transition-metal cluster. Depletion spectra are recorded by monitoring the ratio of the ion intensity for a certain complex with and without FELIX interaction as a function of wavelength. The peak positions of the $\nu(\text{CO})$ bands are determined by a least-squares fit to a Gaussian line shape function. The error is given by the standard deviation (1σ) of the fit. As the detection is mass selective, the simultaneous measurement of IR spectra for different cluster sizes is possible.

III. Results and discussion

We have obtained vibrational spectra for the complexes of a single CO molecule with cationic and neutral Ni clusters, with cationic and anionic Pd clusters, and with cationic, neutral, and anionic Pt clusters. In the case of Ni and Pt, the clusters contain between 3 and 22 atoms. Due to the unfavourable isotope distribution of Pd, its cluster range is limited to 3–12 atoms in the present study. Absorption bands attributable to $\nu(\text{CO})$ are observed in the range of 1550–2100 cm⁻¹ for all clusters. This confirms that CO binds molecularly as a carbonyl ligand in Group 10 clusters at room temperature. Representative depletion spectra comparing anionic palladium and platinum cluster–CO complexes are shown in Fig. 1. It is immediately clear that, while the spectra of the platinum complexes are dominated by a single $\nu(\text{CO})$ peak at relatively high frequency, the spectra of the palladium complexes are significantly more complex with sometimes multiple bands appearing at lower frequency. Bands attributable to μ_1 , μ_2 , and μ_3 sites can be identified, as discussed below. The band

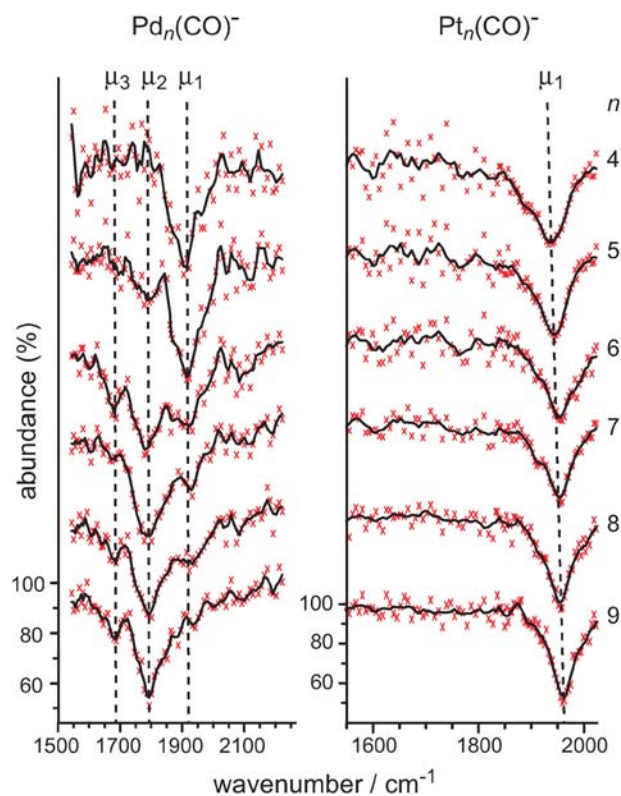


Fig. 1 IR multiple photon dissociation spectra of anionic palladium and platinum cluster–CO complexes, Pd_{*n*}CO⁻ and Pt_{*n*}CO⁻, (*n* = 4–9) in the range of $\nu(\text{CO})$. The crosses represent the raw data while the line interconnects its adjacent three point average. The dashed lines are to guide the eye and indicate the absorption range for atop (μ_1), bridge (μ_2), and hollow sites (μ_3) for palladium and atop sites for platinum. The spectra are offset for clarity.

positions are cluster size dependent and several clusters exhibit CO binding at least at two different sites. As seen in Fig. 2, which presents $\nu(\text{CO})$ as a function of cluster size and charge for all Group 10 metal clusters studied, including previous work of CO adsorption on Ni clusters, this behaviour is repeated in the cations. Unfortunately, anionic nickel clusters and neutral palladium clusters have not been detected in sufficient intensity for IR-MPD spectroscopy but in the case of the cations we can establish a trend from μ_1 binding on Ni clusters to mixed binding including bridge and hollow sites on Pd clusters that is reversed in going to Pt.

A Binding geometries

We determine the binding geometry of CO on metal clusters from $\nu(\text{CO})$ by reference to long-standing experience on surfaces, taking into account that on clusters $\nu(\text{CO})$ is also a function of cluster size and charge. Recently, a quantitative description has been established to model the stretching frequency of CO adsorbed in atop positions¹³ that allows for insights into the bonding interactions. Its main points are briefly summarized. Assuming that the effect of σ -donation does not influence $\nu(\text{CO})$,^{21,20} only π -backdonation and electrostatic effects are taken into account. Electrostatic effects result from an interaction of the dipole of CO with the electric

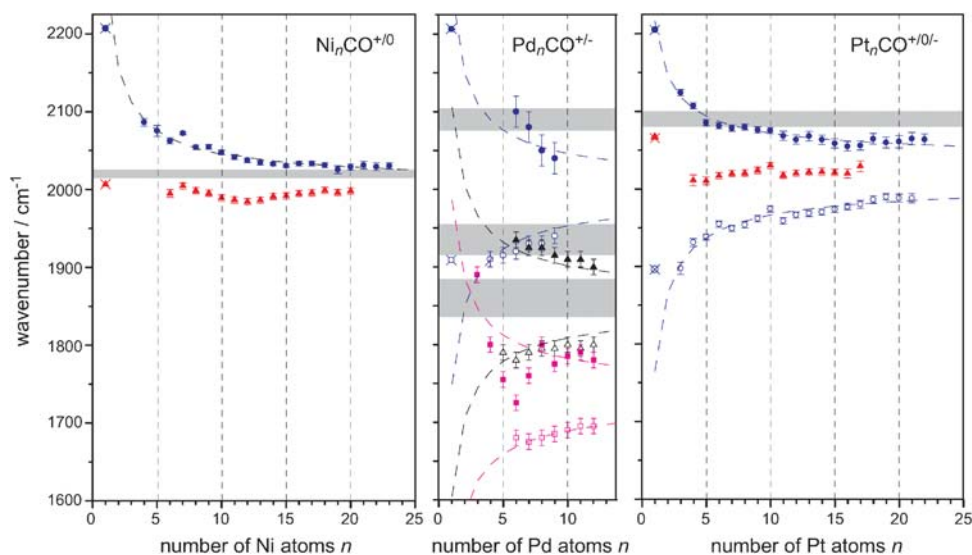


Fig. 2 Frequency of the $\nu(\text{CO})$ vibration in $\text{Ni}_n\text{CO}^{+/0}$ (\bullet) and neutrals (\blacktriangle), $\text{Pd}_n\text{CO}^{+/-}$ (\bullet , \blacktriangle , \blacksquare) and anions (\circ , \triangle , \square), and $\text{Pt}_n\text{CO}^{+/0/-}$ (\bullet), neutrals (\blacktriangle), and anions (\circ) as a function of cluster size. The peak positions are determined by a least-squares fit to a Gaussian line shape function. The error bars indicate the standard deviation (1σ) of the fits. The values of $\nu(\text{CO})$ in the atomic complexes $M\text{CO}^{+/0/-}$ ($M = \text{Ni}, \text{Pd}, \text{Pt}$) are measured in Ne matrices and indicated by crossed symbols.³² The dashed lines in the case of Ni and Pt are the result of a fit to a model that includes electrostatic interaction and π -backdonation; for Pd the dashed lines are the result of the model assuming the values of $\nu_\infty(\text{CO})$ reported in Table 1 (see text for further explanation). The grey bands mark the range of $\nu(\text{CO})$ reported for CO adsorbed at μ_1 sites on the corresponding metal surfaces in the case of nickel^{28,29} and platinum.^{27,34–38} In the case of palladium these bands mark surface values for CO absorbed in μ_1 , μ_2 , and μ_3 sites,^{45–48} in the order of decreasing frequency.

field E induced by the charged cluster. This leads to the following change in $\nu(\text{CO})$:¹³

$$\Delta\nu_{\text{ES}}(\text{CO}) = 1395 \text{ cm}^{-1} \times E/\text{a.u.} \quad (3.1)$$

The electric field E is given by $E = z/r^2$, where z is the charge of the cluster and r the distance from the center of the cluster to the center of the C–O bond.²² It has been shown that electrostatic effects have a significant effect for $\nu(\text{CO})$ of CO adsorbed on transition-metal clusters but that they are not the dominant factor.¹³ The main contribution stems from π -backdonation. For CO bound to a charged metal cluster it can be assumed that the occupancy of the $\text{CO}(2\pi)$ orbital depends linearly on the fraction of the total cluster charge $z \cdot e$ that resides on the metal atom to which the CO binds. Empirically, the best description is based on the assumption that the charge is distributed equally over the cluster surface. Assuming a linear relationship between the $\text{CO}(2\pi)$ orbital occupation and experimental $\nu(\text{CO})$ frequencies, this leads to the following expression for $\nu(\text{CO})$ for atop adsorbed CO on transition-metal clusters:¹³

$$\nu(\text{CO}) = \nu_\infty(\text{CO}) + \Delta\nu_{\text{ES}}(\text{CO}) + \frac{dz}{n_s} \quad (3.2)$$

where n_s is the number of surface atoms. $\nu_\infty(\text{CO})$ is the hypothetical stretching frequency of CO on a cluster with an infinite number of surface atoms. The constant d relates the population of the CO 2π orbital to the CO force constant and can be obtained together with $\nu_\infty(\text{CO})$ by fitting the model to the experimental data. Such fits are shown in Fig. 2 for charged Ni and Pt clusters and they reproduce the experimental findings nicely. For neutral clusters $\nu_\infty(\text{CO})$ is determined as the average value of $\nu(\text{CO})$ for all cluster sizes

measured. The results are summarized in Table 1. Convergence to a common value of $\nu_\infty(\text{CO})$ identifies a common binding site geometry on cationic, neutral, and anionic clusters.

For Ni_2CO and Ni_3CO , vibrationally resolved anion photoelectron spectra reveal rather low values of $\nu(\text{CO})$, $1800 \pm 80 \text{ cm}^{-1}$ and $1750 \pm 80 \text{ cm}^{-1}$, respectively, that suggest the presence of bridging CO ligands.²³ For larger $\text{Ni}_n^{+/0}$ clusters ($n = 5\text{--}23$), $\nu_\infty(\text{CO})$, derived from both the cations and the neutrals, is close to the value attributed to μ_1 binding on Ni surfaces, confirming that we are dealing exclusively with atop binding for the two measured charge states. This is in contrast to nickel surfaces where CO is generally found to bind both in atop and bridge sites.^{24–29} On Ni(111) different studies even exclude CO adsorption in atop positions at low coverage.^{30,31} The preference for atop binding has been attributed to the availability of metal sites with few nearest neighbours on the gas-phase clusters.¹³ Neutral atomic NiCO complexes in neon and argon matrices yield values for the C–O stretch vibration close to $\nu_\infty(\text{CO})$, the value from the argon matrix being $\sim 10 \text{ cm}^{-1}$ more red-shifted than the one from the neon matrix.^{32,33}

The values of $\nu_\infty(\text{CO})$ obtained for CO on anionic, neutral, and cationic Pt clusters lie within less than 25 cm^{-1} from each other. These values are $50\text{--}80 \text{ cm}^{-1}$ lower than the values for CO adsorbed in atop positions on various platinum surfaces but, on the other hand, also at least 140 cm^{-1} higher than the values reported for bridge bound CO.^{27,34–39} The neon-matrix value for cationic Pt^+CO is reproduced by the model while $\nu(\text{CO})$ lies at significantly higher frequencies for the neutral and anionic atomic complexes.³² Note that $\nu(\text{CO})$ for neutral PtCO in an argon matrix yields a value that, again, is shifted to

Table 1 Values for $\nu_{\infty}(\text{CO})$ (in cm^{-1}), deduced from the cluster size dependence of $\nu(\text{CO})$

Metal	Site	$\nu_{\infty}(\text{CO})$			$\nu_{\text{surf}}(\text{CO})^a$
		Anion	Neutral	Cation	
Ni	Atop		1994	2002	2020 ^d
Pd ^c	Atop	2000		2000	2073–2110 ^d
	Bridge	1855		1855	1910–1962 ^d
	Hollow	1735		1735	1830–1895 ^e
Pt	Atop	2012	2020	2035	2083–2100 ^f

^a Values taken from the literature at low CO coverage. ^b For Ni(100) and Ni(911) step sites from ref. 29 and 28. ^c ν_{∞} is the average value for cationic and anionic clusters. ^d For Pd(111) from ref. 45–48. ^e For Pd(111) from ref. 47–49. ^f For Pt(111) from ref. 27 and 34–38.

the red as compared to the neon matrix, this time by 13 cm^{-1} .⁴⁰ It can be concluded that CO binds exclusively atop to the investigated Pt clusters. Based on the high bond dissociation energies for the first three CO ligands as compared to the following ones, molecular orbital arguments, and analogies to organometallic complexes and surface chemistry, it has been argued that CO binds in bridging positions on Pt_3^- .^{41–43} Our findings contradict this tentative interpretation and support instead the predictions based on DFT calculations that CO binds atop to neutral and anionic platinum trimers.⁴⁴

In the case of palladium we can divide the observed values of $\nu(\text{CO})$ into three characteristic groups for both the cationic and anionic complexes. For each charge state these groups can be assigned to CO adsorption atop (blue), bridge (black), and threefold hollow sites (magenta data points in Fig. 2). Although the range of clusters we were able to study is smaller than for the other two metals, it appears from Fig. 2 that each of the three groups converges to a similar value of $\nu_{\infty}(\text{CO})$ for cations and anions. As remarked above, this convergence is characteristic of CO that is adsorbed in the same position. Rather than rely on extrapolation, which is subject to high uncertainty due to the small cluster range and the rather large error in the $\nu(\text{CO})$ band positions, $\nu_{\infty}(\text{CO})$ in Table 1 is obtained differently. Here, $\nu_{\infty}(\text{CO})$ is calculated as the average of $\nu(\text{CO})$ for all cationic and anionic complex pairings for each absorption group. This approach is consistent with eqns (3.1) and (3.2) and is validated by the observation that both methods for obtaining $\nu_{\infty}(\text{CO})$ give similar results for Co, Rh, and Pt clusters. The values of $\nu_{\infty}(\text{CO})$ found for the three groups each correspond to an identified binding geometry on palladium surfaces.^{45–49} The values for the Pd clusters lie around $60\text{--}100 \text{ cm}^{-1}$ below the surface values. This shift is similar to the one found for $\nu_{\infty}(\text{CO})$ of platinum and cobalt cluster cations and the respective surface values, providing support to the assignment of the three groups of $\nu(\text{CO})$ bands to μ_1 , μ_2 , and μ_3 binding.

The presence of more than one absorption band in the spectrum of certain $\text{Pd}_n\text{CO}^{\pm}$ complexes can only be explained by the presence of isomers. These isomers may result from different metal cluster isomers or from a single metal cluster structure, which offers more than one binding site. These two scenarios are difficult to distinguish by spectroscopy alone.¹² On extended palladium surfaces CO shows a tendency to adsorb at a range of coordination sites with the distribution dependent on coverage and temperature, although at low coverage hollow sites are the preferred positions for CO

adsorption.⁵⁰ We already know that certain cluster sizes of rhodium, the second element in Group 9, exhibit CO adsorption in bridge and hollow sites.^{11,12} It seems that coordination in other than atop positions is a characteristic of 4d metal clusters. The reason for this will be discussed below.

B Parallels with surface chemistry and the role of relativistic effects

On extended platinum surfaces, the preference for atop adsorption of CO has been known for a long time. In fact, bridge sites seem to be metastable. Whereas at low temperatures on Pt(111), μ_2 -CO can be observed in the IR spectrum, annealing to 150 K results exclusively in atop-CO, which has been attributed to diffusion of CO from bridge to atop sites.^{27,34} Quantum chemical calculations have difficulties in predicting the atop position as the most stable adsorption site, a phenomenon referred to as “the CO/Pt(111) Puzzle”.^{10,51,52} Empirical corrections, based on the scaling of the singlet–triplet CO excitation energy or of the internal CO stretch vibration, have been implemented in order to find the right adsorption geometries.^{53,54} Furthermore, it has been shown that hybrid functionals with plane-wave basis sets identify the atop position as the most favourable binding site.⁵⁵ With the unambiguous assignment of atop adsorption of CO on small platinum clusters our work provides benchmark data for further theoretical studies.

Calculations on atomic mono-carbonyl complexes and on cluster models for surfaces identify relativistic effects as being behind several aspects of the platinum anomaly.^{8,56} While non-relativistic calculations on the atom–CO complexes show that the M–CO bond length (M = Ni, Pd, Pt) would increase monotonically going from the first to the third row,^{57,58} inclusion of relativistic effects leads to the prediction of a large contraction of the M–CO bond length for platinum compared to only a minor effect for palladium and an almost negligible effect for nickel. This leads to a reversal in the ordering of the M–CO bond length to $\text{Ni} < \text{Pt} < \text{Pd}$ and a considerable strengthening of the Pt–CO bond.^{57,58}

In a work covering the whole nickel group, bridge and atop adsorption sites on an extended surface have been theoretically modeled by eight and nine atom clusters having the structure of small pieces of the bulk crystal.⁸ Using these models the preference of palladium for higher coordinating sites in contrast to platinum’s tendency to bind CO at low coordinating sites has been explained in detail. Without relativistic effects CO molecules would bind the weakest to platinum surfaces and have a strong preference for bridging as compared to atop positions.

Using scalar-relativistic DFT it is observed that the atop adsorption site is stabilized by the above mentioned relativistic contraction of the Pt–C distance, while such a contraction is almost absent for the bridge site.⁸ The reason for this site-dependence lies in the CO 5 σ lone pair. It leads to significant Pauli repulsion with the substrate, which can be reduced upon polarization of the CO 5 σ orbital towards the oxygen atom. At the relativistic level a considerable additional polarization is only possible in the case of atop positions, but not for bridge sites, resulting in less stabilization of the latter one.

This reasoning is fully in line with our vibrational spectra for gas-phase cluster complexes. Based on the experimental observation, one might think that Pd clusters are exceptional, adsorbing CO in bridge, hollow, and atop geometries. However, it is the platinum that behaves out of the ordinary, as the relativistic contraction of the Pt–C bond length leads to a uniquely high stability in case of atop adsorption. The same reasoning would hold also for other late 4d elements and could explain the occurrence of high coordination sites for CO adsorption on rhodium clusters as well.¹² Quantum-chemical calculations for CO adsorption on geometry-optimized clusters of Group 10 elements are still highly desirable for getting quantitative insights in the underlying mechanisms.

C Comparison of gas phase and deposited clusters

Compared to isolated clusters in the gas phase the situation of a cluster on a surface is far more complicated. The interaction between the cluster and the surface can lead to structural rearrangements, the symmetry is reduced, CO adsorption may become sterically hindered, and the electronic properties of the deposited species might change.¹² Still, from the charge dependence of $\nu(\text{CO})$ for a certain cluster size in the gas phase, the charge transfer from the support to the deposited cluster can be estimated.^{12,14} The C–O stretch vibration has been studied on supported particles of known size for all three Group 10 elements.^{59–65}

For Ni₁₁ particles deposited on a MgO-film at 160 K an intense absorption at around 2080 cm⁻¹ has been assigned to atop CO. With rising temperature this band shifts strongly to the red until at 280 K a frequency of 2048 cm⁻¹ is measured.⁵⁹ The gas phase IR-MPD spectra are all measured at 300 K, thus at slightly higher temperature. Furthermore, the isolated cluster complexes each contain exactly one CO molecule, whereas 1–2 CO molecules are estimated to be adsorbed per deposited particle. However, it has been shown that on free rhodium clusters, binding of up to three CO molecules induces only slight shifts of $\nu(\text{CO})$ to the blue.¹² Upon a linear fit of $\nu(\text{CO})$ on neutral and cationic Ni₁₁ clusters, a frequency of 2048 cm⁻¹ translates into a formal charge state of the deposited cluster of about +1.

Better and more complete data for the charge dependence of $\nu(\text{CO})$ is available for free platinum clusters. Fig. 3 presents the charge dependence of $\nu(\text{CO})$ for μ_1 -CO adsorbed on free Pt₈ and Pt₂₀. On Pt₈ and Pt₂₀ supported on a MgO film, atop CO shows absorptions at 2065 and 2045 cm⁻¹, respectively.⁶¹ The formal charge state of the deposited clusters would thus be +0.75 for Pt₈ and +0.6 for Pt₂₀. Again, the exact CO coverage of the deposited clusters is unclear.

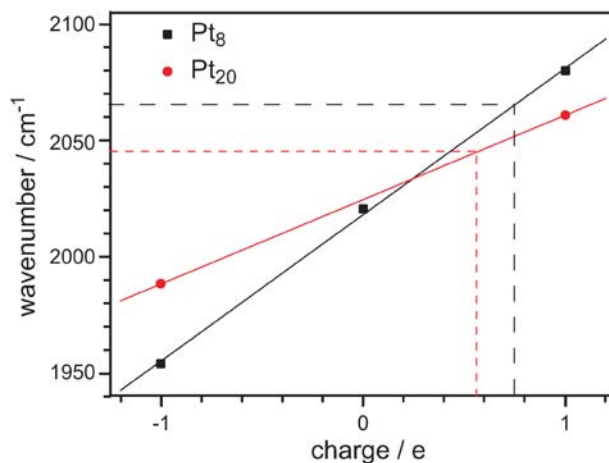


Fig. 3 Charge dependence of $\nu(\text{CO})$ for μ_1 -CO adsorbed on free Pt₈ and Pt₂₀. The dashed horizontal lines indicate values of $\nu(\text{CO})$ of 2065 and 2045 cm⁻¹, which are measured for CO on deposited clusters of the same size.⁶¹ From this graph the partial charges of the deposited clusters can be estimated.

Comparison of $\nu(\text{CO})$ on Group 10 size-selected clusters in the gas phase and supported on MgO reveals a general trend in that $\nu(\text{CO})$ on supported clusters is consistently blue-shifted compared to $\nu(\text{CO})$ of the neutral monoligated species in the gas phase. A slightly higher frequency is expected due to the possibly higher coverage in case of the supported particles. However, this alone cannot explain the substantial blue-shift that is experimentally observed. It therefore seems that the site to which CO adsorbs on the supported particles bears a considerable positive charge. This conclusion has been drawn for all comparisons between gas-phase species and supported clusters on MgO, namely rhodium,¹² nickel, platinum, and gold.¹⁴ In some cases co-adsorption of additional molecules like O₂ or NO could be a reason for the positive charge of the metal. A charge transfer from the support to the metal clusters is possible as well, although it is argued that gold particles prefer electron donating F-centers on the support. Finally, it must be kept in mind that in these studies cationic clusters are deposited and that the clusters might not be fully neutralized after deposition.

IV. Conclusion

IR-MPD spectra have been measured for M_n-CO complexes (M = Ni, Pd, Pt), with *n* up to 22, in various charge states. Clusters of the Group 10 elements all adsorb CO in atop sites, nickel and platinum exclusively. The size and charge dependence of the C–O stretch frequency $\nu(\text{CO})$ can be described by a simple model that includes electrostatic interactions and π -backbonding from the cluster to CO. Palladium binds CO also in bridge and hollow sites. This special behaviour can be understood if modifications in the electronic structures of the complexes due to relativistic effects are taken into account. It is discussed that actually platinum cluster complexes are exceptional because a relativistic contraction of the Pt–CO bond length stabilizes the atop sites in comparison to the bridged sites. Comparison of the charge dependence of $\nu(\text{CO})$

on gas-phase clusters with values of the C–O stretch vibration measured on deposited clusters reveals that supported particles carry a substantial positive charge.

Acknowledgements

We gratefully acknowledge the support of the Stichting voor Fundamenteel Onderzoek der Materie (FOM) in providing beam time on FELIX. The authors thank the FELIX staff for their skilful assistance, in particular Dr B. Redlich and Dr A. F. G. van der Meer. P.G. thanks the IMPRS “Complex Surfaces in Materials Science” for funding.

References

- P. Pyykkö and J. P. Desclaux, *Acc. Chem. Res.*, 1979, **12**, 276.
- P. Pyykkö, *Chem. Rev.*, 1988, **88**, 563.
- H. Schwarz, *Angew. Chem., Int. Ed.*, 2003, **42**, 4442.
- D. J. Gorin and F. D. Toste, *Nature*, 2007, **446**, 395.
- G. C. Bond, *J. Mol. Catal. A: Chem.*, 2000, **156**, 1.
- B. Yoon, H. Häkkinen, U. Landman, A. S. Wörz, J.-M. Antonietti, S. Abbet, K. Judai and U. Heiz, *Science*, 2005, **307**, 403.
- J. P. Desclaux, *Atom. Data Nucl. Data Tables*, 1973, **12**, 311.
- G. Pacchioni, S.-C. Chung, S. Krüger and N. Rösch, *Surf. Sci.*, 1997, **392**, 173.
- P. H. T. Philipsen, E. van Lenthe, J. G. Snijders and E. J. Baerends, *Phys. Rev. B*, 1997, **56**, 13556.
- P. J. Feibelman, B. Hammer, J. K. Nørskov, F. Wagner, M. Scheffler, R. Stumpf, R. Watwe and J. Dumesic, *J. Phys. Chem. B*, 2001, **105**, 4018.
- A. Fielicke, G. von Helden, G. Meijer, B. Simard, S. Dénommée and D. M. Rayner, *J. Am. Chem. Soc.*, 2003, **125**, 11184.
- A. Fielicke, G. von Helden, G. Meijer, D. B. Pedersen, B. Simard and D. M. Rayner, *J. Phys. Chem. B*, 2004, **108**, 14591.
- A. Fielicke, G. von Helden, G. Meijer, D. B. Pedersen, B. Simard and D. M. Rayner, *J. Chem. Phys.*, 2006, **124**, 194305.
- A. Fielicke, G. von Helden, G. Meijer, B. Simard and D. M. Rayner, *J. Phys. Chem. B*, 2005, **109**, 23935.
- A. Fielicke, G. von Helden, G. Meijer, D. B. Pedersen, B. Simard and D. M. Rayner, *J. Am. Chem. Soc.*, 2005, **127**, 8416.
- A. Fielicke, G. von Helden, G. Meijer, B. Simard and D. M. Rayner, *Phys. Chem. Chem. Phys.*, 2005, **7**, 3906.
- D. Oepts, A. F. G. van der Meer and P. W. van Amersfoort, *Infrared Phys. Technol.*, 1995, **36**, 297.
- B. Simard, S. Dénommée, D. M. Rayner, D. van Heijnsbergen, G. Meijer and G. von Helden, *Chem. Phys. Lett.*, 2002, **357**, 195.
- J. Opitz-Coutureau, A. Fielicke, B. Kaiser and K. Rademann, *Phys. Chem. Chem. Phys.*, 2001, **3**, 3034.
- A. J. Lupinetti, S. Fau, G. Frenking and S. H. Strauss, *J. Phys. Chem. A*, 1997, **101**, 9551.
- A. S. Goldman and K. Krogh-Jespersen, *J. Am. Chem. Soc.*, 1996, **118**, 12159.
- The distance r is calculated as $r = r_{\text{Cl}} + r_{\text{C}} + r_{\text{C-O}}/2$, with r_{Cl} and r_{C} being the cluster radius and the covalent radius of a carbon atom in a typical M–C bond, respectively. Note that this formula is erroneous in ref. 13.
- G. Ganteför, G. Schulze Icking-Konert, H. Handschuh and W. Eberhardt, *Int. J. Mass Spectrom. Ion Processes*, 1996, **159**, 81.
- J. Lauterbach, M. Wittmann and J. Kuppers, *Surf. Sci.*, 1992, **279**, 287.
- W. Erley, H. Wagner and H. Mach, *Surf. Sci.*, 1979, **80**, 612.
- S. Haq, J. G. Love and D. A. King, *Surf. Sci.*, 1992, **275**, 170.
- J. Yoshinobu and M. Kawai, *Surf. Sci.*, 1996, **363**, 105.
- K. Sinniah, H. E. Dorsett and J. E. Reutt-Robey, *J. Chem. Phys.*, 1993, **98**, 9018.
- M. Kawai and J. Yoshinobu, *Surf. Sci.*, 1996, **368**, 239.
- J. C. Bertolini and B. Tardy, *Surf. Sci.*, 1981, **102**, 131.
- L. Surnev, Z. Xu and J. T. Yates, *Surf. Sci.*, 1988, **201**, 1.
- B. Liang, M. Zhou and L. Andrews, *J. Phys. Chem. A*, 2000, **104**, 3905.
- H. A. Joly and L. Manceron, *Chem. Phys.*, 1998, **226**, 61.
- J. V. Nekrylova and I. Harrison, *Chem. Phys.*, 1996, **205**, 37.
- K. Y. Kung, P. Chen, F. Wei, Y. R. Shen and G. A. Somorjai, *Surf. Sci.*, 2000, **463**, L627.
- C. Klünker, M. Balden, S. Lehwald and W. Daum, *Surf. Sci.*, 1996, **360**, 104.
- H. Steininger, S. Lehwald and H. Ibach, *Surf. Sci.*, 1982, **123**, 264.
- C. W. Olsen and R. I. Masel, *Surf. Sci.*, 1988, **201**, 444.
- P. Gardner, R. Martin, M. Tüshaus and A. M. Bradshaw, *J. Electron Spectrosc. Relat. Phenom.*, 1990, **54–55**, 619.
- L. Manceron, B. Tremblay and M. E. Alikhani, *J. Phys. Chem. A*, 2000, **104**, 3750.
- A. Grushow and K. M. Ervin, *J. Am. Chem. Soc.*, 1995, **117**, 11612.
- A. Grushow and K. M. Ervin, *J. Chem. Phys.*, 1997, **106**, 9580.
- A. Grushow and K. M. Ervin, *J. Chem. Phys.*, 1997, **107**, 8210.
- T. Santa-Nokki and H. Häkkinen, *Chem. Phys. Lett.*, 2005, **406**, 44.
- V. V. Kaichev, I. P. Prosvirin, V. I. Bukhtiyarov, H. Unterhalt, G. Rupprechter and H. J. Freund, *J. Phys. Chem. B*, 2003, **107**, 3522.
- V. V. Kaichev, M. Morkel, H. Unterhalt, I. P. Prosvirin, V. I. Bukhtiyarov, G. Rupprechter and H. J. Freund, *Surf. Sci.*, 2004, **566–568**, 1024.
- B. Bourguignon, S. Carrez, B. Dragnea and H. Dubost, *Surf. Sci.*, 1998, **418**, 171.
- W. K. Kuhn, J. Szanyi and D. W. Goodman, *Surf. Sci.*, 1992, **274**, L611.
- S. Surnev, M. Sock, M. G. Ramsey, F. P. Netzer, M. Wiklund, M. Borg and J. N. Andersen, *Surf. Sci.*, 2000, **470**, 171.
- M. Tüshaus, W. Berndt, H. Conrad, A. M. Bradshaw and B. Persson, *Appl. Phys. A: Mater. Sci. Process.*, 1990, **51**, 91.
- M. Gajdoš, A. Eichler and J. Hafner, *J. Phys.: Condens. Matter*, 2004, **16**, 1141.
- A. Gil, A. Clotet, J. M. Ricart, G. Kresse, M. García-Hernández, N. Rösch and P. Sautet, *Surf. Sci.*, 2003, **530**, 71.
- S. E. Mason, I. Grinberg and A. M. Rappe, *Phys. Rev. B*, 2004, **69**, 161401.
- F. Abild-Pedersen and M. P. Andersson, *Surf. Sci.*, 2007, **601**, 1747.
- Y. Wang, S. de Gironcoli, N. S. Hush and J. R. Reimers, *J. Am. Chem. Soc.*, 2007, **129**, 10402.
- S.-C. Chung, S. Krüger, S. P. Ruzankin, G. Pacchioni and N. Rösch, *Chem. Phys. Lett.*, 1996, **248**, 109.
- J. Li, G. Schreckenbach and T. Ziegler, *J. Am. Chem. Soc.*, 1995, **117**, 486.
- S.-C. Chung, S. Krüger, G. Pacchioni and N. Rösch, *J. Chem. Phys.*, 1995, **102**, 3695.
- U. Heiz, *Appl. Phys. A: Mater. Sci. Process.*, 1998, **67**, 621.
- A. S. Wörz, K. Judai, S. Abbet and U. Heiz, *J. Am. Chem. Soc.*, 2003, **125**, 7964.
- U. Heiz, A. Sanchez, S. Abbet and W. D. Schneider, *J. Am. Chem. Soc.*, 1999, **121**, 3214.
- T. Dellwig, G. Rupprechter, H. Unterhalt and H. J. Freund, *Phys. Rev. Lett.*, 2000, **85**, 776.
- M. Frank, M. Bäumer, R. Kühnemuth and H. J. Freund, *J. Phys. Chem. B*, 2001, **105**, 8569.
- X. Xu and D. W. Goodman, *Catal. Lett.*, 1994, **24**, 31.
- E. Ozensoy and D. W. Goodman, *Phys. Chem. Chem. Phys.*, 2004, **6**, 3765.